

Manufacture and Characterization of Porous Electrodes Using Graphite Materials

¹Sulistyo, ^{2*}Sri Nugroho, ³Djoeli Satrijo, ⁴Hafiz Rahmat Fikri

^{1,2,3,4}Mechanical Engineering, Diponegoro University, Semarang, Indonesia

*Corresponding Author E-mail: srinugroho@lecturer.undip.ac.id

Abstract - The main challenge in meeting energy needs is balancing demand and supply in addition to the negative impact of energy use on the environment. Currently, most of the energy needs are supplied by fossil fuels whose sources are limited while their demand continues to increase. Efforts to overcome these challenges by developing environmentally friendly energy, one of which is hydrogen energy. One way to get hydrogen is through electrolysis. One of the components of electrolysis is the electrode. The effectiveness of the electrode depends on the surface area, pore structure, and pore distribution. In this paper, we discuss the process of making porous electrodes and determine the effect of porosity on resistivity and compressive strength. The process of making porous electrodes is carried out by adding a pore former with variations of 5%, 10%, and 15% of the total weight of graphite powder, then mixed with a mixer. A homogeneous mixture was added with polyvinyl alcohol as a binder at 4% wt. Powder that has been mixed with polyvinyl alcohol is molded in the form of a cylinder with a pressure of 28 MPa. The green compact was sintered at a temperature of 1200°C with a heating rate of 5°C/min, and a holding time of 1 hour. The sintered product was characterized by porosity, compression, SEM, and resistivity tests. The results showed that the highest compressive strength obtained was 6.809 MPa at a porosity of 27.47% and the highest resistivity was obtained at 0.1757 Ω. meter at a porosity of 39.41%.

Keywords: Electrodes, graphite, pore formers, porosity.

I. INTRODUCTION

The main challenge in meeting energy needs is balancing demand and supply in addition to the negative impact of energy use on the environment [1]. Currently, most of the energy needs are supplied by fossil fuels which can cause environmental problems and the resources are limited, while the demand continues to increase [2]. Efforts to overcome these challenges by developing environmentally friendly energy [3].

Combustion products that are not environmentally friendly as in the combustion process in an internal

combustion engine (ICE) are pollutants, CO₂ and NO_x [4]. These products will cause negative effects on the environment. One of the efforts to obtain environmentally friendly energy is to use hydrogen energy [5]. Hydrogen has a High Heating Value (HHV) of 141.86 KJ/g which is higher than gasoline (47.5 KJ/g) and other solid fuels (50 KJ/g) [6]. If hydrogen energy is used in fuel cell devices, the products produced are electricity, heat, steam (water vapor) and will not produce toxic and dangerous gases [7].

Hydrogen found in nature is not in the form of free elements so it must be processed first. One way to obtain hydrogen is the electrolysis process which produces hydrogen gas [8,9]. Electrolysis is the decomposition of water at the electrodes when an electric field is applied [10]. Electrolysis device components consist of anode, cathode and electrolyte [11]. The schematic of the electrolysis device can be seen in Figure 1 below [11].

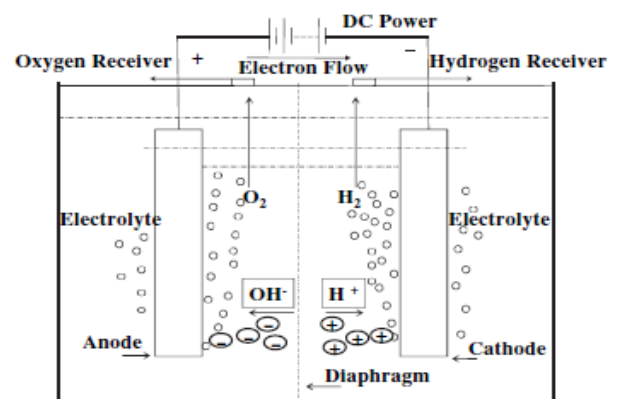
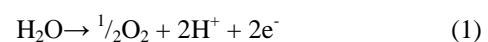
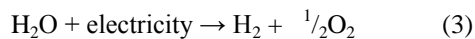


Figure 1: Hydrogen Electrolysis Schematic [11]

In the electrolytic process, at the anode there is a process of decomposition of water into oxygen, the release of 2 H⁺ ions and 2 electrons to the cathode as shown by reaction (1). Meanwhile at the cathode there is a capture of 2 electrons released by the anode so that it will produce hydrogen gas as shown in reaction (2) [12].



Electrolysis of water is not a spontaneous reaction because the overall reaction potential is negative by default. Therefore, external intervention (power source) is needed and the overall electrolysis reaction can be seen in reaction (3) below [13].



The electrolytic process is strongly influenced by the quality of the electrodes. The effectiveness of the electrode depends on the surface area, pore structure, and pore distribution [14]. In general, the porosity of the electrode is an important factor affecting the electrochemical performance, because the available pores determine the effectiveness of the ion intercalation/de-intercalation process [15]. Higher electrode porosity will result in a higher active surface area which will increase the electrochemical reaction.

The reaction that occurs at the electrode is strongly influenced by the material. Considerations for selecting electrode materials are aspects of the manufacturing process, do not react with electrolyte solutions, are resistant to heat, easy to obtain, and cost [16,17]. Based on the condition of the electrode reacting with the electrolyte, the electrode is divided into two types, namely reactive electrodes and inert electrodes. Reactive electrodes are electrodes that participate in reactions with electrolyte solutions which ultimately change the size of the electrode dimensions. Examples of these electrode materials are Copper (Cu), Aluminum (Al), Zinc (Zn), and Iron (Fe) [18]. While the inert electrode is an electrode that does not participate in the reaction so that the dimensions of the electrode are stable and the electrolysis reaction can take place properly. The types of inert electrodes are gold (Au), carbon (C), and platinum (Pt) [19].

Among the three materials, graphite has the highest economic value so it is widely used for various electrochemical applications, one of which is as an electrode material [20]. In addition, graphite is a good conductor, stable at high temperatures and resistant to use. Graphite is an allotrope of carbon which has a crystalline structure. Allotropes are different structural modifications of an element. Graphite has 4 valence electrons of which 3 will be bonded to each other in the form of covalent bonds that are bound in hexagonal lattice sheets [21]. While the other 1 electron floats freely between the various layers of the atom [22]. These electrons act as strong conductors, allowing the electrolysis process to run smoothly.

The embodiment of the electrode material can be carried out by a manufacturing process from the beginning in the form of a powder to a solid electrode. The initial preparation is to choose the size of the graphite powder and the graphite composition. The next step is to carry out the compaction

process at a certain pressure with the desired shape so as to produce a green compact product. In the compaction process, a pore former is added to control the porosity [23]. The pore former will be lost/escaped during the sintering process, resulting in voids on the electrodes [24]. It is expected that the voids formed will produce a void chain. The voids formed are expected to have a homogeneous structure and have a smaller size. The porosity of the electrode material will affect the mechanical and electrical strength [25]. Thus the pore former setting can be done carefully.

The green compact product is followed by a sintering process at a certain temperature. The sintering process is carried out to increase the bonding of powder particles [26,27]. In the sintering process, there is diffusion between atoms to form bonds or compounds in the powder particles. With the increase between atoms will increase the mechanical properties and electrical properties of the electrode [25]. This paper discusses the process of making porous electrodes and characterizing graphite-based electrode materials.

II. METHOD

2.1 Material and specimen preparation

The materials used are graphite powder with a mesh of 100, commercial corn flour with a mesh of 70 as a pore former, and PVA solution as a binder. The equipment used in the manufacture of porous electrodes is mixers, molds, compactors, and furnaces. Before making the porous electrode, the graphite powder was tested for XRF impurities using the Rigaku Supermini 200 tool to determine the impurities present in the graphite powder. The process of making porous electrodes begins by adding a pore former with variations of 5%, 10%, and 15% of the total weight of graphite powder, then mixed using a mixer so that the powder mixture becomes homogeneous. Then the homogeneous powder mixture was added with a 4% wt PVA solution.

2.2 Preparation of specimen

The prepared material is put into a cylindrical mold with a diameter of 7 mm and a length of 160 mm for the compaction process. The pressure applied to the mold is 28 MPa and a green compact product will be produced with a diameter of 7 mm and a length of 49 mm. Then the green compact was sintered with a temperature of 1200°C, heating rate of 5°C/minute, and holding time for 1 hour.

2.3 Characterization

After the porous electrode has been successfully made, characterization is carried out by testing the porosity, compression, and resistivity. The porosity test used in this

study was the Archimedes method with the ASTM C 20-00 standard. ASTM C 20-00 is a technique used to measure porosity by looking at the difference in the weight of the specimen when it is dry and wet. The specimens were dried in a furnace at a temperature of 110°C for 2 hours and then their weight was weighed. After that, the dried specimens were boiled in water for 2 hours and soaked for 12 hours, and then their weight was weighed. The final step is to measure the increase in volume when the specimen is put into a measuring cup filled with water.

$$P = \frac{W_s - W_d}{V_p + V_s} \times 100\% = \frac{V_p}{V_t} \times 100\% \quad (4)$$

Where P is the apparent porosity, W_s is specimen wet weight, W_d is specimen dry weight, V_p is porous volume, V_s is solid volume and V_t is total volume.

Particle crushing strength tests or single compression tests are used to assess the resistance of a graphite electrode to fracture. In this study, the compression test used the ASTM C-695 standard. According to ASTM C-695 there is no general rule for the size of the test specimen, but it has a requirement that the minimum ratio between specimen length and cross-sectional area (width or diameter) must be 1.9 - 2.1 : 1. The graphite electrode sample is pressed between two metal plates, one of which does not move and the second moves downwards in the axial direction at a speed of 1 mm/min using a compression engine mechanical test.

$$C = W/A \quad (5)$$

Where C is compressive strength, W is total load and A is surface area.

The ASTM C611 standard is used in this study for the resistivity test. The resistance is measured using this method. Resistivity data will be derived from the resistance data. The primary distinction between resistance and resistivity is that resistance is influenced by the size of the specimen being measured, but resistivity is unaffected by the specimen's size. The resistivity describes the material's qualities because it is unaffected by size.

$$\rho = (R \times A) / L \quad (6)$$

Where ρ is resistivity, R is specimen resistance, A is surface area, and L is specimen length.

The porosity was determined using the morphological SEM test. Jeol JSM 6510 La is the tool used for morphological SEM testing.

III. RESULT AND DISCUSSION

It is required to examine the composition of the graphite powder material first in order to ascertain the elemental content of the graphite powder material before making the graphite electrode specimen. XRF testing can be used to determine the composition of graphite powder materials. Table 1 shows the findings of XRF composition testing in the form of components.

Table 1: Graphite Powder Element Test Results

Component	Result (%mass)
Al	0,1048
Si	0,5703
P	0,02
S	0,147
K	0,0549
Ca	0,1356
Fe	0,1009
Cu	18,0847
Zn	0,2308
Zr	0,016
Rh	0,1278
Sn	0,1184
Sb	0,7842
Pb	0,5661
C	78,9386

The graphite material utilized as an electrode has an average carbon content of 85.45%, making it appropriate for use as an electrode [28]. Graphite electrodes are created and the sintering procedure is carried out after knowing the composition of the graphite powder material. The electrodes were measured after the sintering process to identify the dimensional changes that happened during the procedure. Before and after the sintering process, the electrode dimensions were measured in Table 2.

Table 2: Measurement of Electrode Dimensions Before and After Sintering

Electrode	Length Before Sintering (mm)	Length After Sintering (mm)	Diameter Before Sintering (mm)	Diameter After Sintering (mm)
Graphite	49	47,97	7	6,8
Graphite+ 5% Pore Former	48,35	46,31	6,8	6,5
Graphite + 10% Pore Former	48,56	46,19	6,9	6,6
Graphite + 15% Pore Former	47.21	45.02	6,6	6

There is dimensional shrinkage in the sintered specimens, according to the data in Table 2. This sintering process is a combustion process that occurs after a molding process in which powder particles are combined through diffusion

processes as the temperature rises, resulting in a stronger and denser product [26]. Water will evaporate during the sintering process, leaving an empty hole that was previously filled with water, resulting in the creation of pores and atomic diffusion [29]. As shown by Roulon's research [30], a binder that is dispersed throughout the compacted powder in a solid form when it reaches the melting point in the sintering process will cause particle rearrangement and shrinkage. PVA (polyvinyl alcohol) is a binder that boils at 228°C [31] and burns entirely at 950°C. The vaporized PVA will leave spaces, allowing diffusion to take place, increasing the density of the material. The specimen dimensions will vary and shrink as a result of this procedure [32]. Figure 2 shows statistics on the porosity of porous electrodes.

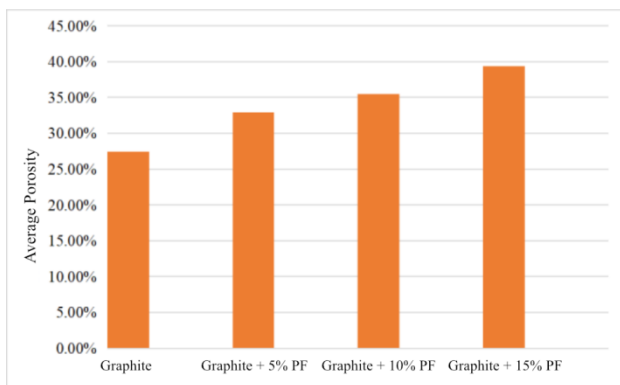


Figure 2: Porosity Graph against the Forming Material

According to Hedayat and Prabowo's research [33,34], the average porosity increases with the number of pore formers. Because the pore former materials are combustible during the sintering process [35], the fewer pore formers used, the fewer voids are produced, and the end product is denser [29]. The porosity of the electrode is kept between 20% and 40% [36] to retain its mechanical strength. This is in line with the findings of the study, which showed a range of 27.47–39.41%.

Figure 3 depicts the porosity aspect of the porous electrode's mechanical strength as indicated by the compressive strength. It shows that the average compressive strength value will decrease along with the increase in the porosity value [37] this is in accordance with research conducted by Dele-Afolabi and Sulisty. [38,39]. The large porosity causes many voids to form, causing the spaces that should be filled with atoms to become empty, resulting in a loss in the specimen's compressive strength [29,40]. This is because the compressive strength of a specimen is proportional to its density; on the other hand, the compressive strength of a specimen is proportional to its density [41].

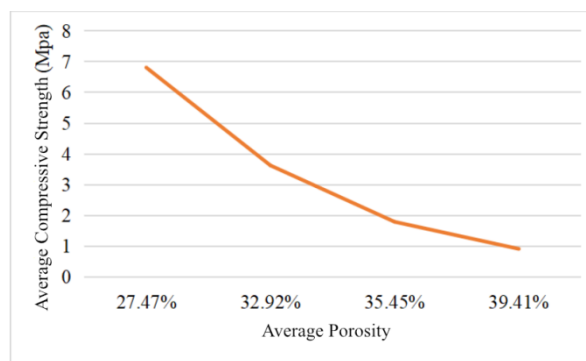


Figure 3: Compressive Strength against the Porosity Graph

After measuring the porosity and compressive strength, it was discovered that the pores had a significant impact on the values of porosity and compressive strength [40]. In order to back up the results of the porosity and compressive tests, the SEM test was carried out to show the pores produced on the electrode's surface. The porous electrode's SEM morphological examination findings are shown in Figure 4. The red arrow in Figure 4 indicates the vacant area of the graphite electrode that is not filled with particles and generates a porosity. In the graphite electrode SEM morphology, few pores form without the application of a pore creator, as shown in Figure 4(a). SEM testing on graphite electrodes with pore formers is used to observe the changes that occur. When a pore former is introduced to a graphite electrode, it causes macro pores to grow on the electrode but not micropores, resulting in a change in the graphite electrode's structure [42]. The space between the graphite electrode particles widens as the pore former is increased. The sintering process, which burns the pore shape of corn flour at a temperature of roughly 600 oC, causes this state. Corn flour burns and vanishes, leaving holes (pores). More holes were produced as more corn flour was applied to the graphite electrode [39]. When a 5 percent pore former is added to Figure 4 (b), fewer pores are generated, however when a 15 percent pore former is added to Figure 4 (d), more and more uniform pores are formed. The higher the relative porosity of a material, the more gaps are generated between the particles, and the particle bond chains become more tenuous. Because the bonding support between one particle and another is so weak, the material's strength falls as it becomes less dense. [39].

The resistivity and porosity of the porous electrode are shown in Figure 5. Along with the porosity, the resistivity value will rise. Montes' research [44] supports this conclusion. Carbon materials' porosity is recognized to have an impact on their resistivity value. Quantitative models of the relationship between porosity and electrical resistivity in carbon materials, on the other hand, are still missing [45]. This is related to the resistivity's nature, which rises in lockstep with porosity. Because of the channel produced by the pores, the greater the

porosity, the smaller the part of the electric current transfer and the longer the path that must be crossed [44].

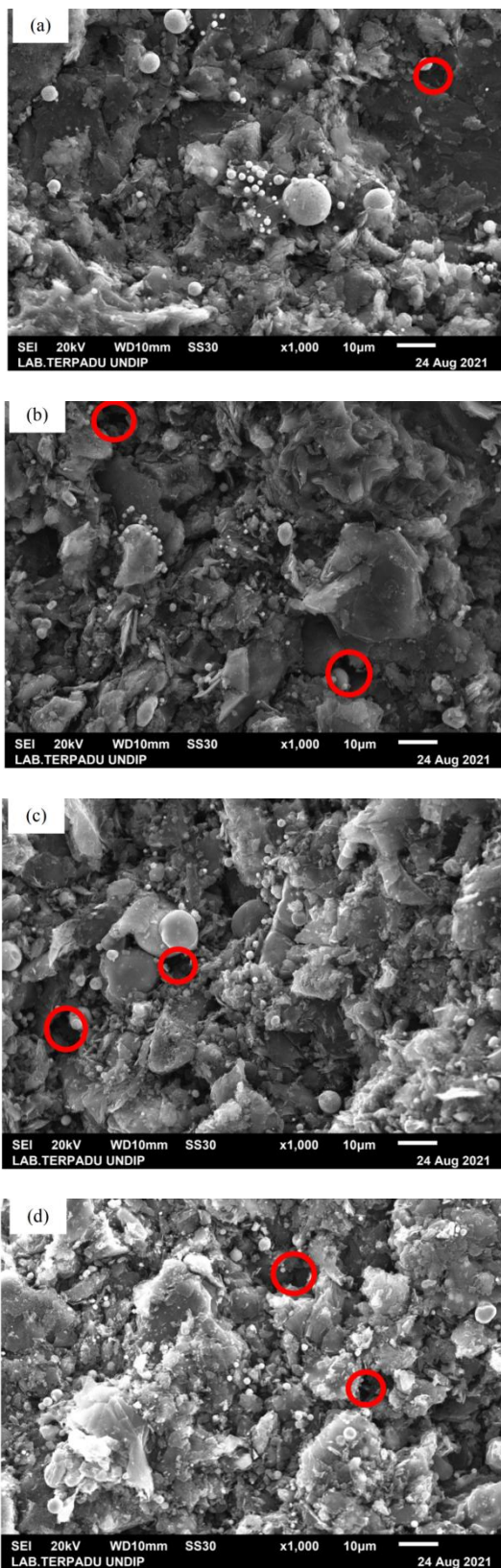


Figure 4: Porous Graphite Electrode Morphology (a) Without Addition of Pore Former (b) Addition of Pore Former 5% (c) Addition of Pore Former 10% (d) Addition of Pore Former 15%

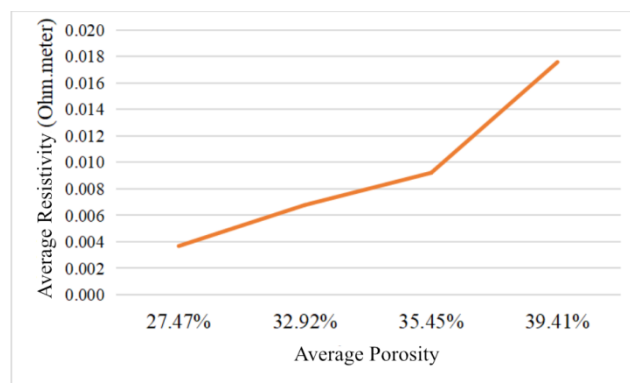


Figure 5: Resistivity Graph against the Porosity

IV. CONCLUSION

According to the study's findings, the porosity rose in tandem with the quantity of pore formers applied. Because the pore former materials are combustible during the sintering process [35], the fewer pore formers used, the fewer voids produced, and the end product is denser. The morphology of the SEM porous electrode revealed the formation of porosity. Porosity has an effect on compressive strength; for example, when porosity increases, the average compressive strength drops. Because of the high value of porosity, many voids arise; leaving the gaps that should be filled with atoms vacant. As a result, the specimen's compressive strength is reduced. The resistivity value will grow as the porosity value at the electrode increases. This is related to the resistivity's nature, which will rise in tandem with the increase in porosity. Because of the channel produced by the pores, the greater the porosity, the smaller the portion of the electric current transfer and the longer the path that must be crossed [44].

REFERENCES

- [1] Hosseini SE, Andwari AM, Wahid MA, Bagheri G. A review on green energy potentials in Iran. *Renew Sustain Energy Rev* 2013;27:533–45. <https://doi.org/10.1016/j.rser.2013.07.015>.
- [2] Uysal S, Kaya MF, Demir N, Hüner B, Özcan RU, Erdem ÖN, et al. Investigation of hydrogen production potential from different natural water sources in Turkey. *Int J Hydrogen Energy* 2021;46:31097–107. <https://doi.org/10.1016/j.ijhydene.2021.07.017>.
- [3] Ishaq H, Dincer I. Comparative assessment of renewable energy-based hydrogen production methods. *Renew Sustain Energy Rev* 2021;135:110192. <https://doi.org/10.1016/j.rser.2020.110192>.
- [4] Miyamoto T, Hasegawa H, Mikami M, Kojima N, Kabashima H, Urata Y. Effect of hydrogen addition to intake gas on combustion and exhaust emission characteristics of a diesel engine. *Int J Hydrogen Energy* 2011;36:13138–49. <https://doi.org/10.1016/j.ijhydene.2011.06.144>.
- [5] Rievaj V, Gaňa J, Synák F. Is hydrogen the fuel of the future? *Transp Res Procedia* 2019;40:469–74.

- <https://doi.org/10.1016/j.trpro.2019.07.068>.
- [6] Chi J, Yu H. Water electrolysis based on renewable energy for hydrogen production. *Cuihua Xuebao/Chinese J Catal* 2018;39:390–4. [https://doi.org/10.1016/S1872-2067\(17\)62949-8](https://doi.org/10.1016/S1872-2067(17)62949-8).
- [7] Jamrozik A, Grab-Rogaliński K, Tutak W. Hydrogen effects on combustion stability, performance and emission of diesel engine. *Int J Hydrogen Energy* 2020;45:19936–47. <https://doi.org/10.1016/j.ijhydene.2020.05.049>.
- [8] Givirovskiy G, Ruuskanen V, Ojala LS, Lienemann M, Kokkonen P, Ahola J. Electrode material studies and cell voltage characteristics of the in situ water electrolysis performed in a pH-neutral electrolyte in bioelectrochemical systems. *Heliyon* 2019;5:e01690. <https://doi.org/10.1016/j.heliyon.2019.e01690>.
- [9] Sui J, Chen Z, Wang C, Wang Y, Liu J, Li W. Efficient hydrogen production from solar energy and fossil fuel via water-electrolysis and methane-steam-reforming hybridization. *Appl Energy* 2020;276:115409. <https://doi.org/10.1016/j.apenergy.2020.115409>.
- [10] Liyanage D, Walpita J. Organic pollutants from E-waste and their electrokinetic remediation. *INC*; 2019. <https://doi.org/10.1016/B978-0-12-817030-4.00006-1>.
- [11] Ursúa A, Gandía LM, Sanchis P. Hydrogen production from water electrolysis: Current status and future trends. *Proc IEEE* 2012;100:410–26. <https://doi.org/10.1109/JPROC.2011.2156750>.
- [12] Dossow M, Dieterich V, Hanel A, Spliethoff H, Fendt S. Improving carbon efficiency for an advanced Biomass-to-Liquid process using hydrogen and oxygen from electrolysis. *Renew Sustain Energy Rev* 2021;152:111670. <https://doi.org/10.1016/j.rser.2021.111670>.
- [13] Naimi Y, Antar A. Hydrogen Generation by Water Electrolysis. *Intech* 2018:1–18.
- [14] Taspika AM. Manufacture of Porous Carbon Capacitor Electrodes From Pecan Shells (Aleurites Moluccana) As Capacitive Deionization System. *J Fis Unand* 2015;4:173–7. <https://doi.org/10.25077/jfu.4.2>.
- [15] Yermukhambetova A, Berkinova Z, Golman B. Characterization of porous structure of graphite electrode with different packing densities. *Mater Today Proc* 2019;18:487–93. <https://doi.org/10.1016/j.matpr.2019.06.235>.
- [16] Kim WY, Son DJ, Yun CY, Kim DG, Chang D, Sunwoo Y, et al. Performance assessment of electrolysis using copper and catalyzed electrodes for enhanced nutrient removal from wastewater. *J Electrochem Sci Technol* 2017;8:124–32. <https://doi.org/10.5229/JECST.2017.8.2.124>.
- [17] Zhang B, Zhang SX, Yao R, Wu YH, Qiu JS. Progress and prospects of hydrogen production: Opportunities and challenges. *J Electron Sci Technol* 2021;19:1–15. <https://doi.org/10.1016/J.JNLEST.2021.100080>.
- [18] Hayati S, Kurniasih Y. The Effect of Types Materials Electrode on the Efficiency of Silver Electrodeposition from Waste Photontgen 2020:210–5.
- [19] Afiah S. Study of Electrical Power Characteristics of Seawater With Voltaic Cell Principle and Electrode Corrosion Effects. *Universitas Hasanudin*, 2017.
- [20] Tetra Olly, Aziz Hermansyah, Emriadi, Ibrahim Sanusi AA. Review: Supercapacitors Based on Activated Carbon and Ionic Solutions as Electrolytes. *J Zarah* 2018;6:39–46.
- [21] Rahman DY. Efficiency Improvement Of Grafit / Tio2 Based Solar Cells Through Deposition Of Mineral Ions And Optimization Of Lioh Concentration In Polymer Electrolyte. *Bandung Institute Technology*, 2019.
- [22] Simbolon AH. Performance of graphite/graphene, mn/graphite and mn/graphene as electrodes on primary stamped anode. *Universitas Sumatera Utara*, 2018.
- [23] Drożdż E, Stachura M, Wyrwa J, Rękas M. Effect of the addition of pore former. *J Therm Anal Calorim* 2015;122:157–66. <https://doi.org/10.1007/s10973-015-4693-y>.
- [24] Schmidt CG, Andersen KB, Stamate E, Kaiser A, Hansen KK. The role of pore-formers on grain interior and grain boundary conductivity in tape-cast porous sheets for electrochemical flue gas purification. *J Ceram Sci Technol* 2017;8:485–92. <https://doi.org/10.4416/JCST2017-00024>.
- [25] Guler O, Bagci N. A short review on mechanical properties of graphene reinforced metal matrix composites. *J Mater Res Technol* 2020;9:6808–33. <https://doi.org/10.1016/j.jmrt.2020.01.077>.
- [26] Callister WD, Rethwisch DG. *Materials Science and Engineering An Introduction*. 8th ed. New York: Wiley; 2011. <https://doi.org/10.1063/1.2982126>.
- [27] Black JT, Kohser RA. *De Garmo's Materials and Processes in Manufacturing*. John Wiley & Sons; 2020. <https://doi.org/10.1201/b11792-12>.
- [28] Taer E, Afrianda A, Apriwandi, Taslim R, Agustino A, Awitdrus, et al. Production of activated carbon electrodes from Sago waste and its application for an electrochemical double-layer capacitor. *Int J Electrochem Sci* 2018;13:10688–99. <https://doi.org/10.20964/2018.11.27>.
- [29] Sulisty S. Impact of Ceramic Material Sintering Process on Mechanical Properties and Dimensions of a Product. *Rotasi* 2018;20:244. <https://doi.org/10.14710/rotasi.20.4.244-248>.
- [30] Roulon Z, Missiaen J-M, Lay S. Shrinkage and microstructure evolution during sintering of cemented carbides with alternative binders. *Int J Refract Met Hard Mater* 2021;101:105665. <https://doi.org/10.1016/j.jrmhm.2021.105665>.
- [31] Aslam M, Kalyar MA, Raza ZA. Polyvinyl alcohol: A review of research status and use of polyvinyl alcohol based nanocomposites. *Polym Eng Sci* 2018;58:2119–32. <https://doi.org/10.1002/pen.24855>.
- [32] Fergus J, Hui R, Xianguo L, Wilkinson D, Zhang J. *Solid Oxide Fuel Cells: Materials Properties and Performance*. 2008.
- [33] Hedayat N, Du Y, Ilkhani H. Pyrolyzable pore-formers for the porous-electrode formation in solid oxide fuel cells: A review. *Ceram Int* 2018;44:4561–76. <https://doi.org/10.1016/j.ceramint.2017.12.157>.
- [34] Prabowo A, Fadli A, Komalasari. The Effect of Corn Starch Addition on Bone Prototyping Using the Starch

- Consolidation Method. Jom FTEKNIK 2019;6:1–6.
- [35] Rahayu I. Manufacture and characterization of ceramic membranes with variations of rice flour as an additive to the microfiltration process. *J Sains Dan Terap Kim* 2017;11:52. <https://doi.org/10.20527/jstk.v11i2.4035>.
- [36] Wincewicz KC, Cooper JS. Taxonomies of SOFC material and manufacturing alternatives. *J Power Sources* 2005;140:280–96. <https://doi.org/10.1016/j.jpowsour.2004.08.032>.
- [37] Kinasih TAP, Darmawan ADP, Ramadhan RF, Utama W. Analysis of the Effect of Porosity on Compressive Strength Values of Andesite Rocks Using Matlab-Based Hasselman And Ryshkevitch Regression Models. *J Fis Indones* 2020;24:131. <https://doi.org/10.22146/jfi.v24i3.56549>.
- [38] Dele-Afolabi TT, Hanim MAA, Norkhairunnisa M, Sobri S, Calin R. Investigating the effect of porosity level and pore former type on the mechanical and corrosion resistance properties of agro-waste shaped porous alumina ceramics. *Ceram Int* 2017;43:8743–54. <https://doi.org/10.1016/j.ceramint.2017.03.210>.
- [39] Sulistyoyo. Quality Control of Anode Solid Oxide Fuel Cell (SOFC) Through Porosity Control. *Semin Nas Tah Tek Mesin Indones XIV* 2015:7–8.
- [40] Mahdiana N, Arifi E, Wisnumurti W, Firdausy AI. Effect of Void Ratio and Permeability of Concrete on the Compressive Strength of Porous Concrete with RCA. *Rekayasa Sipil* 2018;12:134–41. <https://doi.org/10.21776/ub.rekayasasipil.2018.012.02.9>.
- [41] Sultan MA, Imran, Litolily F. Correlation of porosity of concrete to average compressive strength. *Teknologi Sipil* 2018;2:57–63.
- [42] Ahmad SH, Jamil SM, Othman MHD, Rahman MA, Jaafar J, Ismail AF. Pore former addition in the preparation of highly porous anode using phase-inversion technique for solid oxide fuel cell. *J Membr Sci Res* 2019;5:268–73. <https://doi.org/10.22079/JMSR.2018.74729.1162>.
- [43] Hakamada M, Kuromura T, Chen Y, Kusuda H, Mabuchi M. Influence of porosity and pore size on electrical resistivity of porous aluminum produced by spacer method. *Mater Trans* 2007;48:32–6. <https://doi.org/10.2320/matertrans.48.32>.
- [44] Montes JM, Cuevas FG, Cintas J, Ternero F, Caballero ES. Electrical Resistivity of Powdered Porous Compacts. *Intech* 2018:1–24.
- [45] Sun TM, Dong LM, Wang C, Guo WL, Wang L, Liang TX. Effect of porosity on the electrical resistivity of carbon materials. *Xinxing Tan Cailiao/New Carbon Mater* 2013; 28:349–54. [https://doi.org/10.1016/S1872-5805\(13\)60087-6](https://doi.org/10.1016/S1872-5805(13)60087-6).

Citation of this Article:

Sulistyoyo, Sri Nugroho, Djoeli Satrijo, Hafiz Rahmat Fikri, “Manufacture and Characterization of Porous Electrodes Using Graphite Materials” Published in *International Research Journal of Innovations in Engineering and Technology - IRJIET*, Volume 6, Issue 11, pp 84-90, November 2022. Article DOI <https://doi.org/10.47001/IRJIET/2022.611010>
